Journal of Zhejiang University-SCIENCE B (Biomedicine & Biotechnology) *2023 24(3):207-220*
www.jzus.zju.edu.cn; www.springer.com/journal/11585
E-mail: jzus_b@zju.edu.cn

Research Article

https://doi.org/10.1631/jzus.B2200405

Disulfiram enhances the antitumor activity of cisplatin by inhibiting the Fanconi anemia repair pathway

Meng YUAN[1*], Qian WU[2*], Mingyang ZHANG[2], Minshan LAI[2,3], Wenbo CHEN[2,3], Jianfeng YANG[4,5], Li JIANG[6✉], Ji CAO[2,6,7✉]

[1]*Laboratory of Fruit Quality Biology / the State Agriculture Ministry Laboratory of Horticultural Plant Growth, Development and Quality Improvement, Fruit Science Institute, College of Agriculture and Biotechnology, Zhejiang University, Hangzhou 310058, China*
[2]*Institute of Pharmacology and Toxicology, Zhejiang Province Key Laboratory of Anti-Cancer Drug Research, College of Pharmaceutical Sciences, Zhejiang University, Hangzhou 310058, China*
[3]*Polytechnic Institute, Zhejiang University, Hangzhou 310015, China*
[4]*Department of Gastroenterology, Affiliated Hangzhou First People's Hospital, Zhejiang University School of Medicine, Hangzhou 310006, China*
[5]*Key Laboratory of Integrated Traditional Chinese and Western Medicine for Biliary and Pancreatic Diseases of Zhejiang Province, Hangzhou 310006, China*
[6]*The Innovation Institute for Artificial Intelligence in Medicine, Zhejiang University, Hangzhou 310018, China*
[7]*Cancer Center of Zhejiang University, Hangzhou 310058, China*

Abstract: A series of chemotherapeutic drugs that induce DNA damage, such as cisplatin (DDP), are standard clinical treatments for ovarian cancer, testicular cancer, and other diseases that lack effective targeted drug therapy. Drug resistance is one of the main factors limiting their application. Sensitizers can overcome the drug resistance of tumor cells, thereby enhancing the antitumor activity of chemotherapeutic drugs. In this study, we aimed to identify marketable drugs that could be potential chemotherapy sensitizers and explore the underlying mechanisms. We found that the alcohol withdrawal drug disulfiram (DSF) could significantly enhance the antitumor activity of DDP. JC-1 staining, propidium iodide (PI) staining, and western blotting confirmed that the combination of DSF and DDP could enhance the apoptosis of tumor cells. Subsequent RNA sequencing combined with Gene Set Enrichment Analysis (GSEA) pathway enrichment analysis and cell biology studies such as immunofluorescence suggested an underlying mechanism: DSF makes cells more vulnerable to DNA damage by inhibiting the Fanconi anemia (FA) repair pathway, exerting a sensitizing effect to DNA damaging agents including platinum chemotherapy drugs. Thus, our study illustrated the potential mechanism of action of DSF in enhancing the antitumor effect of DDP. This might provide an effective and safe solution for combating DDP resistance in clinical treatment.

Key words: Disulfiram (DSF); Cisplatin (DDP); DNA damage; Fanconi anemia (FA) repair; Chemotherapy

1 Introduction

Platinum drugs, such as cisplatin (DDP) and oxaliplatin, are widely used in the clinical treatment of various cancers. The antitumor effect of platinum drugs is related to their inhibitions of DNA synthesis. After entering the cell, DDP can bind DNA through the interaction of the platinum atom and the N7 position of purine bases, leading to the formation of intra-strand and inter-strand crosslinks. These DNA cross-links induce disruption of the DNA double helix and block DNA replication and transcription (Brabec and Nováková, 2006). They also increase the level of oxidation in the tumor, which in turn causes cell death. Although DDP is highly efficient, intrinsic resistance and resistance acquired during treatment cycles are relatively common and remain a major challenge for DDP-based anticancer therapy (Rocha et al., 2018; Makovec, 2019; Yang et al., 2021). Therefore, there is an urgent need to find an effective platinum-based drug sensitization regimen to increase patient survival.

✉ Ji CAO, caoji88@zju.edu.cn
Li JIANG, jiangli49@zju.edu.cn
* The two authors contributed equally to this work
Ji CAO, https://orcid.org/0000-0003-2813-6404
Li JIANG, https://orcid.org/0000-0003-4890-1206

Received Aug. 11, 2022; Revision accepted Nov. 1, 2022;
Crosschecked Feb. 22, 2023

Chemotherapeutic drugs exert anti-cancer efficacy by triggering DNA damage, but activation of DNA damage repair (DDR) pathways to counteract the DNA damage serves as one major mechanism of chemoresistance. It has been suggested that a primary cause of platinum resistance is the recovery of the Fanconi anemia (FA) repair pathway. The FA pathway is a stepwise protein network comprising 20 complementation groups and associated genes. Key steps in the pathway include the post-translational modifications of FA complementation group D2 (FANCD2) and FA complementation group I (FANCI), assembly of the FA core complex, and interstrand crosslink-mediated repair of damaged DNA (Smogorzewska et al., 2007; Castella et al., 2015). Monoubiquitination of FANCD2 and its binding partner of FANCI, which is regulated by the ataxia telangiectasia-mutated (ATM)-Rad3-relater kinase (ATR), plays an important role in triggering FA activation (Ishiai, 2021).

During cancer treatment, the FA pathway is abnormally active in cancer cells, helping them to avert or overcome DNA damage induced by drugs. Yarde et al. (2009) found that overexpression of the *FA* gene is correlated with the chances of further drug resistance to DNA alkylating agents in myeloma patients. This suggests that inhibitors of the FA pathway may be an alternative therapy to increase the efficacy of anticancer drugs.

There have been some studies of platinum-based sensitization regimens. It has been reported that monocrystalline iron oxide nanoparticles (MIONs) can enhance the sensitivity of DDP-resistant ovarian cancer, increasing the level of intracellular reactive oxygen species (ROS) and reducing the level of glutathione (Min et al., 2010). The combination of the mammalian target of rapamycin complex 1/2 (mTORC1/2) inhibitors AZD8055 and DDP can significantly enhance DDP-induced apoptosis in testicular cancer (Zhao et al., 2014; Nakano et al., 2021). Moreover, metformin can improve the efficacy of DDP in the treatment of non-small cell lung cancer, breast cancer, and other cancers, and may be involved in different regulatory mechanisms (Lee et al., 2019; Guo et al., 2021; Liang et al., 2021). Although these schemes propose a drug combination strategy to potentially sensitize the antitumor activity of DDP, most of the sensitizing compounds used are drug candidates in preclinical research and therefore are unsuitable for rapid clinical application. To accelerate clinical application, we conducted research using the marketed drug library and found that the combination of disulfiram (DSF) and DDP can significantly enhance cytotoxicity (Schmidtova et al., 2019; Yang et al., 2019; Jangra et al., 2020).

DSF (tetraethylthiuram disulfide, Antabuse) is a safe and inexpensive alcohol withdrawal drug (20–40 USD per 250 mg) discovered in the 19th century and used mainly for the treatment of chronic alcoholism. In the 1970s, a 38-year-old breast cancer patient with bone metastases survived for another ten years after quitting all treatments, and tumor tissue that had metastasized to the bones magically disappeared. It was concluded that this was due to long-term intake of DSF for alcoholism, which suggested that DSF may also have antitumor effects. Additionally, a study involving a database of 240 000 tumor patients indicated that those who continued to take DSF had a 34% reduction in mortality rate compared to those who did not (Skrott et al., 2017). A growing number of preclinical studies have proved that DSF can have significant antitumor activity.

As reported, DSF in combination with Cu sensitizes DDP by targeting aldehyde dehydrogenase-positive ($ALDH^+$) cells. DSF/Cu inhibits the P-glycoprotein drug efflux pump to enhance the antitumor activity of paclitaxel (Wang et al., 2021). In addition, DSF/Cu may interfere with the proteasome to sensitize cells to temozolomide and reduce nuclear factor-κB (NF-κB) activity to retard inhibitor of NF-κB (IκB) degradation, thereby heightening the sensitivity of tumor cells to gemcitabine (Kita et al., 2019; Halatsch et al., 2021). Furthermore, DSF/Cu reverses doxorubicin resistance by increasing c-Jun NH_2-terminal kinase (JNK) expression and phosphorylation (Xu et al., 2020). More importantly, as an adjuvant of antitumor drugs, various clinical trials have been conducted to evaluate the effects of DSF in non-small cell lung cancer, liver cancer, breast cancer, pancreatic cancer, and others, which have further demonstrated the synergistic effect of DSF and chemotherapeutics for oncotherapy (Park et al., 2018; Liu et al., 2021; Ren et al., 2021). Recently, DSF's copper metabolite, bis-diethyldithiocarbamate-copper complex (CuET), was shown to be responsible for DSF antitumor activity by targeting nuclear protein localization protein 4 (NPL4) (Skrott et al., 2017, 2019). However, these studies focused mainly on the copper complex

or metabolite of DSF and indicated that DSF functions as a copper ionophore to mediate antitumor efficacy (Chen et al., 2021). In our previous study, we found that in the absence of copper, DSF enhanced the antitumor activity of *N*-(4-hydroxyphenyl) retinamide (4-HPR) (Wu et al., 2022). Therefore, the synergistic antitumor effect of DSF needs to be explored in depth.

In this study, we aimed to identify marketable drugs that could be potential chemotherapy sensitizers and explore the underlying mechanisms. We found that the alcohol withdrawal drug DSF could significantly enhance the antitumor activity of DDP. Further research tends to explain how DSF works in enhancing the antitumor activity of DDP. We hope that the mechanism we discovered could be used as a theoretical basis for clinical DDP and DSF treatment options.

2 Materials and methods

2.1 Antibodies and reagents

Antibodies against phosphorylated histone H2AX (γH2AX; #9718s) and cleaved caspase-3 (#9664) were obtained from Cell Signaling Technology (Boston, USA). Antibodies against cleaved-poly(ADP-ribose) polymerase (c-PARP; ET1608-10), FANCD2 (ET1611-67), excision repair cross-complementation group 1 (ERCC1; ET1703-19), and phospho-ATM (S1981; ET1705-50) were obtained from Hua'an Biotechnology (Hangzhou, China). Antibodies against FANCI (#ab245219) were obtained from Abcam (Cambridge, England). Antibodies against glyceraldehyde-3-phosphate dehydrogenase (GAPDH; #db106) and β-actin were from Diage Bio (Hangzhou, China). Adriamycin, DDP, mitomycin C, and geldanamycin were obtained from Topscience (Shanghai, China). Benzyloxycarbonyl-Val-Ala-Asp-fluoromethylketone (Z-VAD(OMe)-FMK; T6013), hydroxyurea, oxaliplatin (T0164), and carboplatin (T1058) were obtained from TargetMol (Shanghai, China). JC-1 (M8650) was obtained from Solarbio (Beijing, China), DSF (T110101) from Aladdin (Hangzhou, China), and propidium iodide (PI; ZF-50-0001) from Multi Science (Shanghai, China).

2.2 Cell culture

H1299, Bel-7402, HCT116, HCC1937, SW1990, and PANC-1 cell lines were purchased from the Shanghai Institute of Biochemistry and Cell Biology (Shanghai, China) and were authenticated by short tandem repeat (STR) profiling. PANC-1 cells were cultured in Dulbecco's modified Eagle medium (DMEM) high glucose medium (12800, Gibco, USA). H1299, Bel-7402, HCC1937, and SW1990 cells were cultured in RPMI-1640 medium (31800, Gibco, USA). HCT116 cells were cultured in McCoy's 5A medium (M4892, Sigma-Aldrich, USA). All media were supplemented with 10% (0.1 g/mL) fetal bovine serum (SV30160.03, HyClone, USA). The cells were maintained in a humidified atmosphere of 5% CO_2 at 37 °C.

2.3 Proliferation inhibition assay

Cells were seeded at an appropriate density in 96- or 6-well plates. After 24 h, dimethyl sulfoxide (DMSO) or other compounds were added to the wells and the plates were incubated for 48 or 72 h. Medium was removed and cells were fixed with 10% (0.1 g/mL) trichloroacetic acid for 1 h and stained with sulforhodamine B (SRB; #S1402, Sigma-Aldrich, St. Louis, MO, USA) for 30 min at room temperature, after which the excess dye was washed repeatedly with 1% (volume fraction) acetic acid. The protein bound dye was then dissolved in 10 mmol/L Tris-base solution. The absorbance of SRB was measured at 510 nm using a microplate reader (Tecan, Spark, Switzerland). The cell proliferation inhibition rate was calculated as a percentage of the proliferation rate of the negative control treatment.

2.4 JC-1 staining

For staining, cells were washed with phosphate-buffered saline (PBS) and resuspended in 500 μL staining solution containing 1× JC-1 monomer (M8650, Solarbio, China) and incubated at 37 °C for 15 min. The samples were then centrifuged at 500*g* for 5 min at room temperature. After the supernatant was discarded and the cells resuspended in 300 μL PBS, the samples were ready to be analyzed. Cell fluorescence was recorded by a flow cytometer (Beckman Coulter, USA) equipped with a 488-nm excitation laser. Data were collected from the phycoerythrin (PE)/fluorescein isothiocyanate (FITC) dual channel (575 nm/525 nm). At least 10 000 cells were collected for each group and analyzed using FlowJo 7.6 software (FlowJo, BD Bioscience, USA).

2.5 Western blot analysis

Cell lysates were prepared as described previously (Wu et al., 2022). The proteins were separated on sodium dodecyl sulfate-polyacrylamide gel electrophoresis (SDS-PAGE) gels and transferred to polyvinylidene fluoride (PVDF) membranes (#00010, Millipore, Bedford, MA, USA) using the Bio-Rad blotting system. The membranes were blocked with 5% (0.05 g/mL) non-fat milk and incubated with different primary antibodies at 4 ℃ overnight. The membranes were then incubated with horseradish peroxidase (HRP)-conjugated secondary antibody for 1 h at room temperature. The proteins were visualized using an enhanced chemiluminescence (ECL) detection kit (NEL103E001EA, PerkinElmer, USA) with an AI680 imager (Cytiva, USA). Gray scale analysis was performed using ImageJ software (1.52A-Java-1.8.0-261, NIH, USA).

2.6 RNA sequencing

Tumor cells at an appropriate density were seeded in 100 mm×100 mm petri dishes for drug treatment. After that, 1–2 mL TRIzol (#AL42091A, TaKaRa Bio Inc., Japan) was added to fully lyse the cells, and then samples were sent to the Shanghai Bohao Biotechnology Co., Ltd. (Shanghai, China) for detection and analysis.

2.7 Immunofluorescence

Slides, 14 mm×14 mm, were loaded into the bottom of a 24-well plate, and then the cells were seeded at an appropriate density for drug treatment. After sufficient time, the culture medium was discarded and the slides were washed three times with 1× PBS, 5 min each time, then fixed with 500 μL 4% (volume fraction) paraformaldehyde at room temperature for 20 min, and washed three times with PBS. A total of 500 μL 1× PBS containing 0.4% (volume fraction) TritonX-100 and 2% (volume fraction) bovine serum albumin (BSA) was used to block at room temperature for 30 min, followed by washing three times with PBS. Then 300 μL immunofluorescent primary antibody diluted with PBS of 0.1% (volume fraction) Triton X-100 and 0.5% (volume fraction) BSA in the volume ratio of 1∶400 or 1∶800 was added, and the slides were placed in a horizontal shaker overnight at 4 ℃. After washing three times with PBS, 300 μL immunofluorescence secondary antibody was added, diluted in the volume ratio of 1:400 (the buffer solution is the same as above), and incubated at room temperature in the dark for 1 h before being washed three times with PBS. Finally, the cells were fixed on the slides with 4',6-diamidino-2-phenylindole (DAPI) sealing agent, and dried and photographed under different channels of the fluorescent confocal microscope.

2.8 PI staining

Cells were washed once with cold PBS and resuspended with 750 μL cold absolute ethanol followed by 250 μL sterile PBS to a total volume of 1 mL and fixed overnight at −20 ℃. After being centrifuged at 1800 r/min for 5 min, 500 μL PBS containing 2.5 μL RNase was added and the slides were incubated at 37 ℃ for 30 min. Then 5 μL PI dye was added and the slides were kept in darkness for 10 min at room temperature. The samples were then analyzed. Cell fluorescence was recorded using a flow cytometer (Beckman Coulter) equipped with a 488-nm excitation laser. Data were collected from PE single channel (525 nm). At least 10000 cells were collected for each treatment condition and the analysis was carried out using FlowJo 7.6 software.

2.9 Statistical analysis

All cell proliferation inhibition experiments were analyzed using Prism 8.0 (GraphPad software, USA) and results are shown as mean±standard deviation (SD). Immunofluorescence statistics were analyzed using ImageJ analysis software, and the average number of foci in each cell was calculated. ImageJ software was used to analyze the gray value of each strip. A *t*-test or analysis of variance (ANOVA) was used to analyze the differences between groups. When $P<0.05$, differences were considered significant.

3 Results

3.1 Synergistic antitumor effect of DSF and DDP

To identify a candidate for resolving platinum drug resistance, we screened the drug library and found that DSF and DDP showed a significant synergistic enhancement of the antitumor effect on different cancer cell lines (Fig. 1). However, DSF made no difference to the inhibition of proliferation induced by other chemotherapeutics like adriamycin, mitomycin C, geldanamycin, paclitaxel, gemcitabine, and

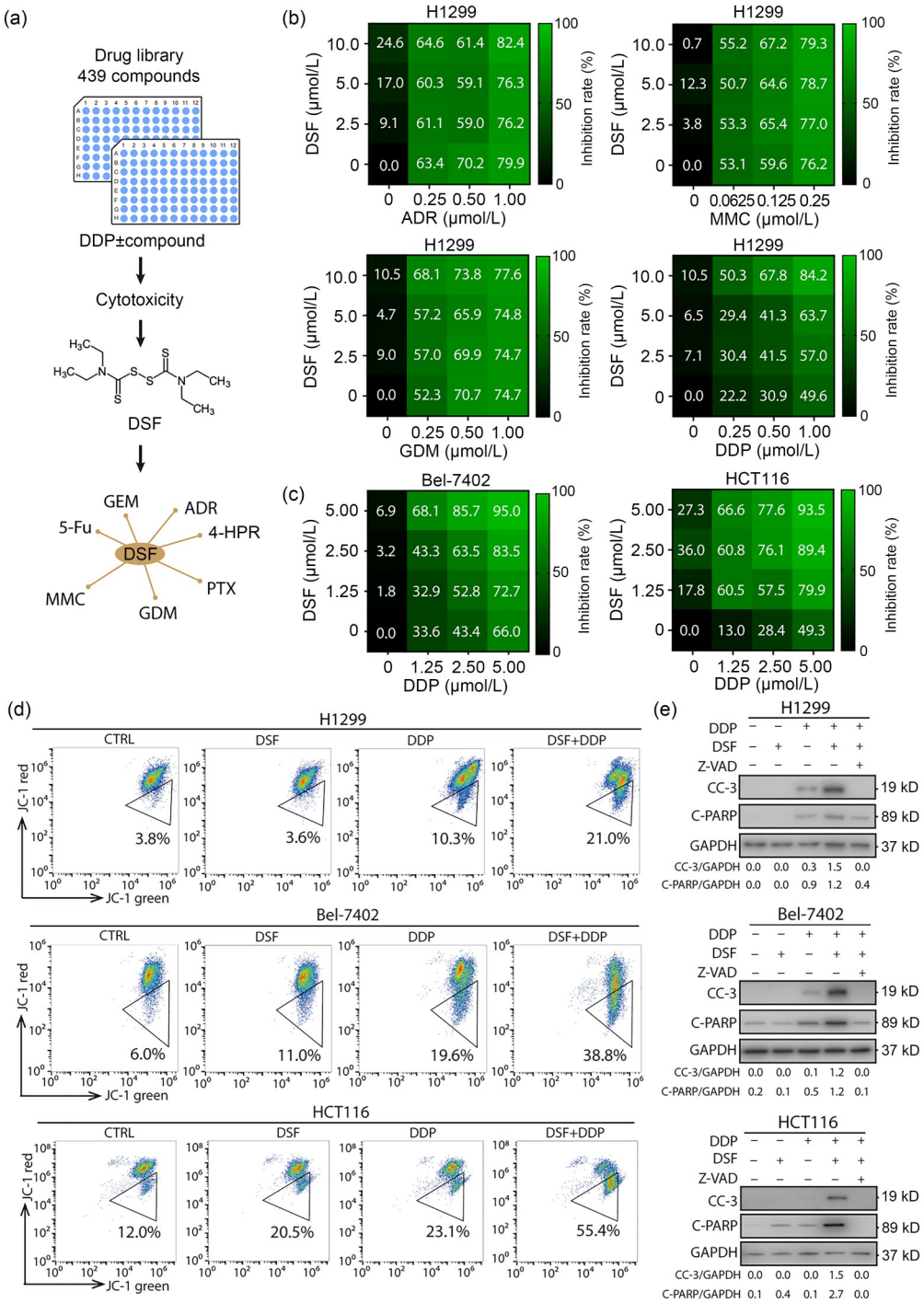

Fig. 1 Synergistic antitumor effect of DSF and DDP. (a) A flow chart of the drug screening process; (b) H1299 cells were treated with DSF and ADR, MMC, GDM, or DDP alone or simultaneously at different concentrations for 72 h and examined by the SRB assay; (c) Bel-7402 and HCT116 cells were treated with DSF and DDP alone or simultaneously at different concentrations for 72 h and examined by the SRB assay; (d) H1299 and Bel-7402 cells were treated with 5 μmol/L DSF and 5 μmol/L DDP alone or simultaneously for 48 h, and HCT116 cells were treated for 24 h; (e) H1299, Bel-7402, and HCT116 cells were treated with 5 μmol/L DSF, 5 μmol/L DDP, and 20 μmol/L Z-VAD alone or simultaneously for 72, 48, and 24 h, respectively. Western blot was performed with antibodies against C-PARP and CC-3. DSF: disulfiram; DDP: cisplatin; ADR: adriamycin; MMC: mitomycin C; GDM: geldanamycin; GEM: gemcitabine; PTX: paclitaxel; 5-FU: 5-fluorouracil; 4-HPR: *N*-(4-hydroxyphenyl) retinamide; SRB: sulforhodamine B; CTRL: control; C-PARP: cleaved-poly(ADP-ribose) polymerase; Z-VAD: benzyloxycarbonyl-Val-Ala-Asp; CC-3: cleaved caspase-3; GAPDH: glyceraldehyde-3-phosphate dehydrogenase.

5-fluorouracil (5-FU) (Figs. 1b, 1c, and S1a). We introduced a combination index (CI) value to identify the synergy of DSF and DDP. We used the 50% inhibition rate to calculate the CI values. A combination of 5 μmol/L DSF and 5 μmol/L DDP applied to three types of tumor cells produced CI values ranging from 0.7 to 0.1 (Fig. S1b), indicating that DSF plus DDP had a synergistic antitumor effect. Therefore, we used 5 μmol/L DSF plus 5 μmol/L DDP for further studies. Stronger proliferation inhibition was also observed in the DSF and DDP combination group in H1299, Bel-7402, and HCT116 cells (Fig. S1c). Moreover, DSF showed only mild inhibition of cell proliferation in normal cells at high concentration (Fig. S1d), suggesting its safety in antitumor regimens.

DDP damages tumors mainly via induction of apoptosis (Bai et al., 2022). Accordingly, H1299, Bel-7402, and HCT116 cells were treated with 5 μmol/L DSF and 5 μmol/L DDP alone or in combination, and then apoptosis was detected via JC-1 staining. The proportion of early apoptosis in the combination treatment group was increased compared to that of the individual treatment group in H1299 cells (3.8% in the control group, 3.6% in the DSF treatment group, 10.3% in the DDP treatment group, and 21.0% in the combined treatment group; Fig. 1d). The apoptosis-sensitizing effect of DSF on DDP was also apparent in the Bel-7402 and HCT116 cells. Apoptosis can cause cleavages of PARP and caspase-3. Therefore, western blots were prepared (Fig. 1e). Accumulation of c-PARP and caspase-3 suggested that stronger apoptosis occurred in cells of the combination treatment group. Moreover, Z-VAD-FMK (Z-VAD), a pan-caspase inhibitor, could reverse this apoptosis, which suggested that DSF might amplify the DDP-induced antitumor effect mainly via the apoptosis pathway.

3.2 Effect of DSF on the DDP-induced DNA damage

Some studies have shown that the antitumor activity of DSF depends mainly on the ROS generated after its introduction or complexing of its reduction product with intracellular divalent metal ions (Yang et al., 2019). Previous data (Fig. 1b) also showed that up to 10 μmol/L DSF did not cause obvious cytotoxicity. We assumed that DSF could exert a synergistic antitumor effect in a metal ion-independent manner, indicating that an unknown molecular mechanism might account for its antitumor effect. Therefore, we applied RNA sequencing, which technic has been widely used in oncology (Qi et al., 2021; Zhong et al., 2021; Xia et al., 2022), to discover the potential mechanism. For RNA sequencing, we set up four groups of cells with different treatment conditions: DMSO alone (control group), 5 μmol/L DSF and 5 μmol/L DDP alone or simultaneously. The sequencing results were analyzed according to the following steps: firstly, the fold changes (logarithm with base 2, $\log_2$FC) of every gene were calculated compared to the control group. Then we selected those genes that were virtually unchanged in the DSF treatment group, but more variable (up- or down-regulated) in the combination treatment group than in the DDP treatment group. A total of 6703 genes were obtained (Fig. 2a). We found plenty of DDR-related genes were significantly down-regulated among the 6703 genes (Fig. 2b). Subsequently, Gene Set Enrichment Analysis (GSEA) was performed based on the differential genes (Fang et al., 2022), and relevant pathways were selected according to the criteria of a P value less than 0.05 and a q value less than 0.25. We found that in response to DNA damage stress, the cyclin D1, activating transcription factor 2 (ATF2), and ATM signaling pathways were more activated in the combination treatment group compared to the DDP treatment group (Fig. 2c). These results indicated that the sensitizing effect of DSF on DDP might be related to the augmentation of DNA damage.

Based on the results of GSEA pathway enrichment analysis, we conducted cell biology experiments for validation. We first evaluated the formation of γH2AX nuclear foci by immunofluorescence, which is indicative of induction of double-strand DNA breakage, in H1299 and Bel-7402 cells treated with 5 μmol/L DSF and 5 μmol/L DDP alone or simultaneously for 24 h. As expected, there were no significant γH2AX foci after DSF treatment, while DDP induced the formation of γH2AX foci. Additionally, the γH2AX foci increased in the combination treatment group, indicating that DNA damage was exacerbated cumulatively (Fig. 2d). We also detected other representative markers of DNA damage such as phosphorylated ATM via western blot on Bel-7402 and HCT116 cell lines treated with 5 μmol/L DSF and 5 μmol/L DDP alone or simultaneously for 48 h. The ATM phosphorylation was more up-regulated in the combination treatment group (Fig. 2e). These results were consistent with those of

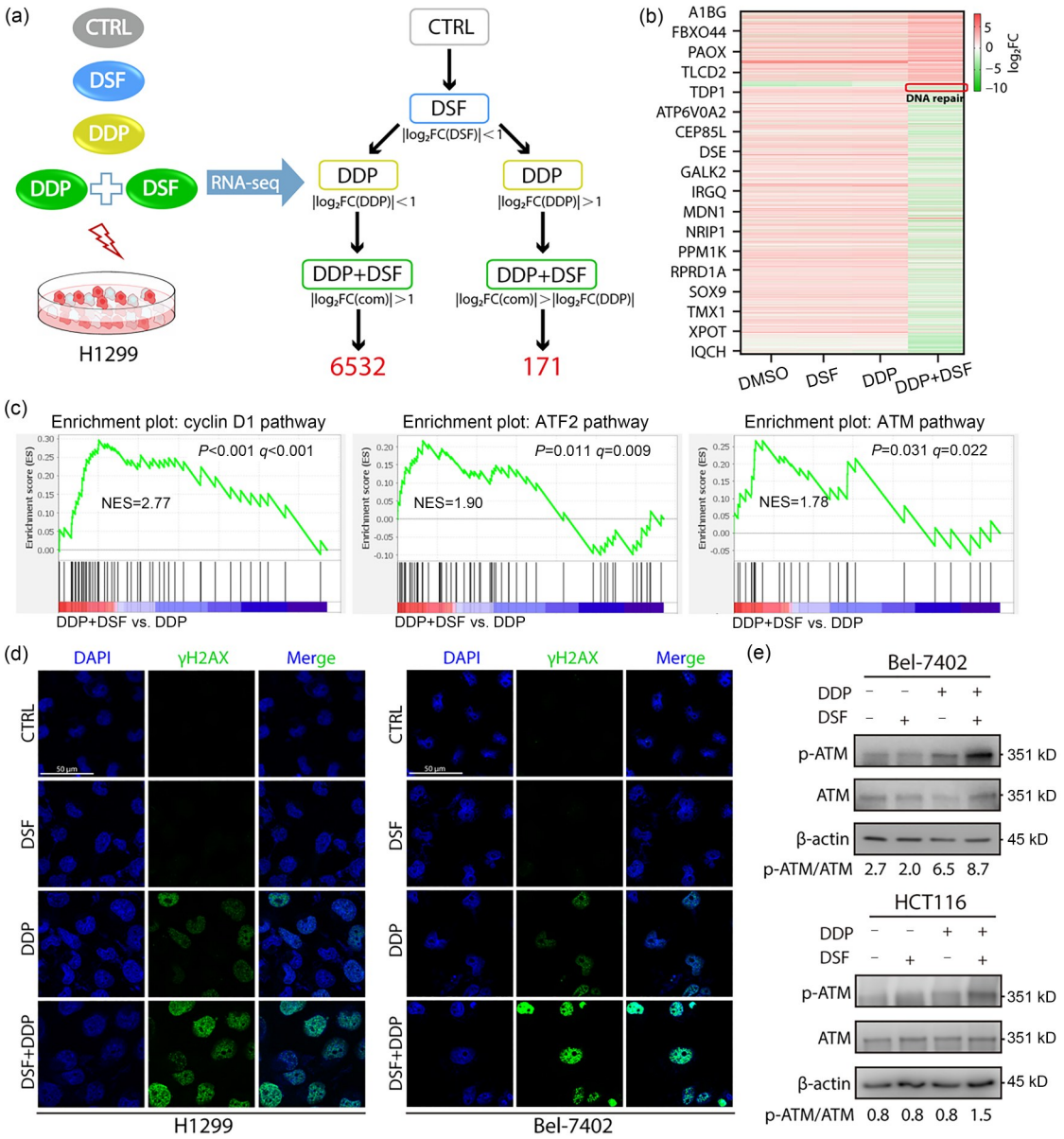

Fig. 2 DSF can enhance DDR induced by DDP to mediate the synergistic effect. (a) H1299 cells treated with 5 μmol/L DDP and 5 μmol/L DSF alone or simultaneously for 48 h and analyzed by RNA-seq. A total of 6703 genes were chosen, which were virtually unchanged in the DSF treatment group, but more significantly variable in the combination treatment group than in the DDP treatment group. (b) Among the 6703 genes, many genes associated with DDR were down-regulated in the combination treatment group. (c) GSEA pathway enrichment analysis of 6703 differential genes showed that the cyclin D1, ATF2, and ATM signaling pathways were more activated in the combination treatment group. (d) Representative pictures of γH2AX foci in H1299 and Bel-7402 cells with four different treatment conditions: vehicle 24 h+vehicle 24 h, 5 μmol/L DSF 24 h+vehicle 24 h, 5 μmol/L DDP 24 h+vehicle 24 h, and 5 μmol/L DDP 24 h+5 μmol/L DSF 24 h. (e) The changes of the phosphorylation levels of ATMs in Bel-7402 and HCT116 cells, and results were analyzed using ImageJ. CTRL: control; DSF: disulfiram; DDP: cisplatin; RNA-seq: RNA sequencing; DDR: DNA damage repair; FC: fold change; com: combination; DMSO: dimethylsulfoxide; A1BG: α-1B-glycoprotein; FBXO44: F-box protein 44; PAOX: polyamine oxidase; TLCD2: TLC domain containing 2; TDP1: tyrosyl-DNA phosphodiesterase 1; ATP6V0A2: ATPase H^+ transporting V0 subunit A2; CEP85L: centrosomal protein 85-like; DSE: dermatan sulfate epimerase; GALK2: galactokinase 2; IRGQ: immunity-related GTPase Q; MDN1: midasin AAA ATPase 1; NRIP1: nuclear receptor interacting protein 1; PPM1K: protein phosphatase, Mg^{2+}/Mn^{2+}-dependent 1K; RPRD1A: regulation of nuclear pre-NRNA domain-containing 1A; SOX9: SRY-box transcription factor 9; TMX1: thioredoxin-related transmembrane protein 1; XPOT: exportin for TRNA; IQCH: IQ motif-containing H; GSEA: Gene Set Enrichment Analysis; ATF2: activating transcription factor 2; ATM: ataxia telangiectasia-mutated; NES: normalized enrichment score; γH2AX: phosphorylated histone H2AX; DAPI: 4',6-diamidino-2-phenylindole; p-: phosphorylated.

immunofluorescence, showing that the combination of DSF and DDP could increase DNA damage in tumor cells. The above data verified the result of GSEA pathway enrichment analysis and supported the hypothesis that the synergistic antitumor effect of DSF was exerted by enhancing DNA damage induced by DDP.

3.3 Effect of DSF on FA repair pathway activated by DDP

Generally, DNA damage caused by cross-linking between DDP and DNA is repaired mainly through the FA repair and nucleotide excision repair (NER) pathways (Feng et al., 2021). We investigated which of these pathways was influenced by DSF. FANCD2 and FANCI are vital elements of the FA core complex in the FA repair pathway, and ERCC1 takes part in the NER pathway. Thus, we first examined the formation of FANCD2 and FANCI foci in H1299 and Bel-7402 cells treated with 5 μmol/L DSF and 5 μmol/L DDP alone or simultaneously. The treatment of DDP triggered the formation of FANCD2 and FANCI foci in H1299 cells, while this phenomenon was diminished in the combination treatment group (Figs. 3a and 3b). Statistical analysis of the confocal photographs showed that, compared with the DDP treatment group, the numbers of foci of FANCD2 and FANCI in the DDP and DSF combined treatment group were reduced by 84% and 64%, respectively (Figs. 3c and 3d). Similarly, in Bel-7402 cells the numbers of FANCD2 and FANCI foci in the DDP and DSF combined treatment group were reduced by 41% and 53%, respectively (Figs. S2a–S2d). However, we found that no ERCC1 foci formed in the four groups, indicating that the combined DDP and DSF treatment did not affect the NER pathway in H1299 or Bel-7402 cells (Figs. 3e and S2e).

As proved, the FA repair pathway acts in a cell cycle-dependent manner and generally occurs in the S or G2 phase. Moreover, DDP can arrest the cell cycle in the S or G2/M phase. To examine whether DSF might indirectly inhibit the FA repair pathway by intervening in the cell cycle, we treated H1299 and Bel-7402 cells with 5 μmol/L DSF and 5 μmol/L DDP alone or simultaneously and analyzed the cell cycle using PI staining. In H1299 cells, the proportion of cells in G2/M phase was 18.7% in control group, 17.1% in the DSF treatment group, 36.7% in the DDP treatment group, and 31.6% in the combined treatment group (Fig. 3f). A similar response was apparent in Bel-7402 cells (Fig. S2f). These results showed that DSF had no effect on enhancing the cycle arrest caused by DDP. The above results (Figs. 3a–3d and S2a–S2d) suggested that DSF may not directly affect the FA repair pathway, but may cause a block upstream of it, thereby decreasing the FANCD2 and FANCI foci rather than indirectly inhibiting the FA repair pathway by affecting the cell cycle.

3.4 Sensitizing effect of DSF on DNA damage agents depending on FA repair

As key factors of the FA repair pathway, FANCD2 and FANCI proteins form heterodimers, which are recruited to DNA after ubiquitination, and form nuclear foci in damaged cells undergoing DNA damage. To confirm the inhibitory effect of DSF on the FA repair pathway, we examined the monoubiquitylation levels of FANCD2 and FANCI in H1299 and Bel-7402 cells treated with 5 μmol/L DSF and 5 μmol/L DDP alone or simultaneously for 24 h. Then, the ratios of monoubiquitinated to non-ubiquitinated form were calculated by grayscale analysis (-L for monoubiquitin modification and -S for non-ubiquitinated form). DDP significantly resulted in increased monoubiquitylation of FANCD2 and FANCI, while DSF down-regulated the monoubiquitin modification of the two proteins in H1299 cells (the ratios of FANCD2-L/S and FANCI-L/S were 0.26, 0.27, 0.70, 0.30 and 0.11, 0.13, 0.40, 0.24 in the control group, DSF treatment group, DDP treatment group, and combination group, respectively) and Bel-7402 cells (the ratios of FANCD2-L/S and FANCI-L/S were 0.06, 0.07, 0.61, 0.45 and 0.02, 0.06, 0.41, 0.27 in the control group, DSF treatment group, DDP treatment group, and combination group, respectively) (Fig. 4a). Taken together, these results indicated that sensitization of tumor cells to DDP by DSF resulted from enhanced DDP-induced DNA damage by inhibition of the FA repair pathway.

Based on this finding, we speculated that DSF might sensitize other DNA damage agents which mainly activate the FA repair pathway. Therefore, we introduced the second-generation platinum-based drug carboplatin and the third-generation platinum-based drug oxaliplatin that, like DDP, disrupt DNA function by binding to DNA. We examined the effects of DSF on the antitumor activities of carboplatin and oxaliplatin.

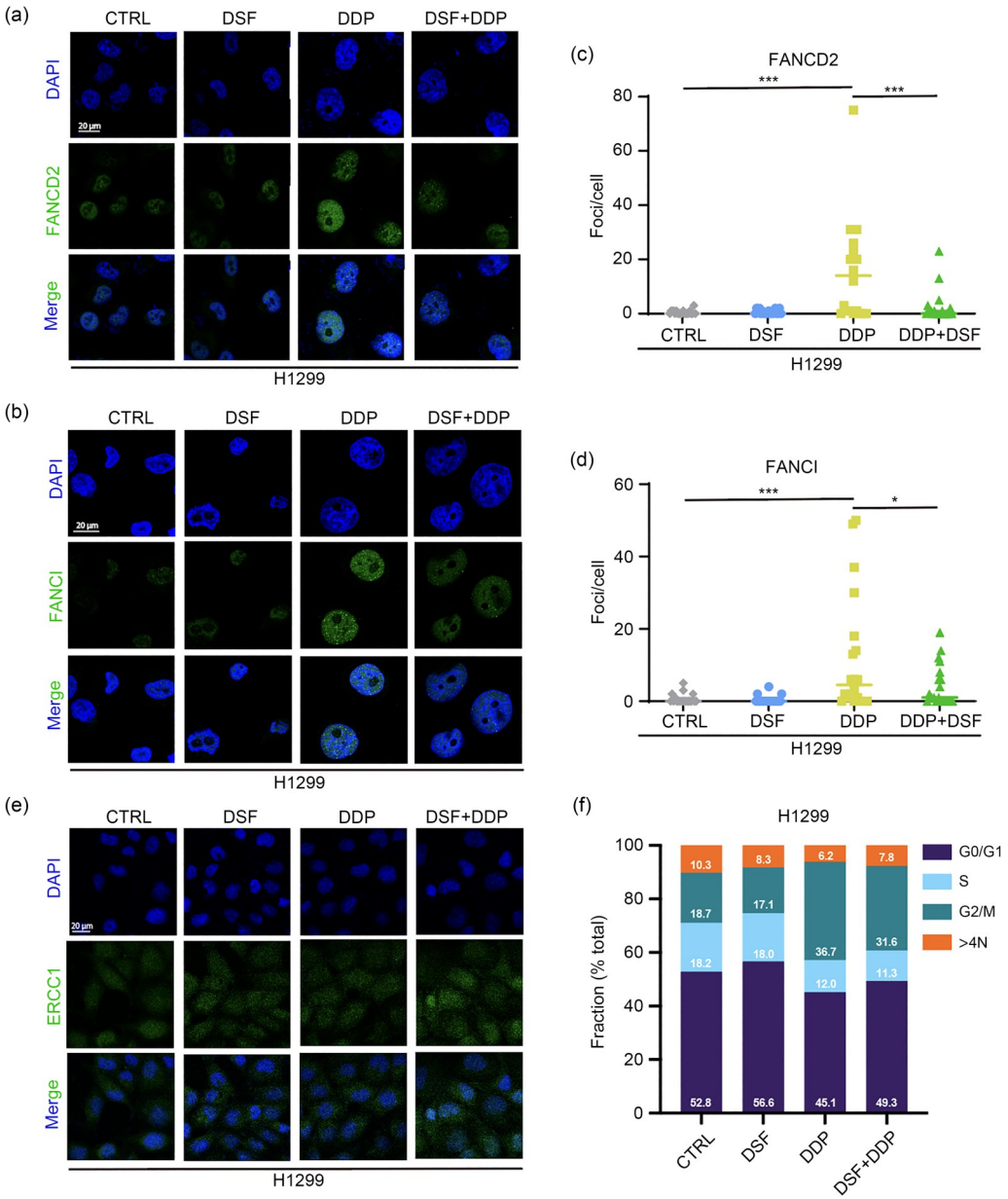

Fig. 3 Inhibitory effect of DSF on the FA repair pathway activated by DDP. (a, b) Representative pictures of FANCD2 (a) and FANCI (b) foci in H1299 cells treated with four treatment conditions: vehicle 24 h+vehicle 24 h, 5 μmol/L DSF 24 h+vehicle 24 h, 5 μmol/L DDP 24 h+vehicle 24 h, and 5 μmol/L DDP 24 h+5 μmol/L DSF 24 h. (c, d) Quantification of FANCD2 (c) and FANCI (d) foci shown in (a) and (b), respectively. Foci in different pictures were counted using ImageJ, n=20 (*** P<0.001, * P<0.05, vs. DDP group). (e) Representative photos of ERCC1 foci in H1299 cells treated with four treatment conditions: vehicle 24 h+vehicle 24 h, 5 μmol/L DSF 24 h+vehicle 24 h, 5 μmol/L DDP 24 h+vehicle 24 h, and 5 μmol/L DDP 24 h+5 μmol/L DSF 24 h. (f) H1299 cells were treated with 5 μmol/L DSF and 5 μmol/L DDP alone or simultaneously for 36 h, and the cell cycle was detected by PI staining. CTRL: control; DSF: disulfiram; DDP: cisplatin; FA: Fanconi anemia; FANCD2: FA complementation group D2; FANCI: FA complementation group I; DAPI: 4',6-diamidino-2-phenylindole; PI: propidium iodide.

H1299 cells were treated with 5 μmol/L DSF and 10 μmol/L carboplatin or 10 μmol/L oxaliplatin alone or simultaneously for 48 h and then cell viabilities were tested by SRB assay. DSF significantly increased proliferation inhibition caused by carboplatin (0.4% in the DSF-treating group, 11.5% in the carboplatin-treating group, and 44.5% in the combination-treating group) and oxaliplatin (2.8% in the DSF-treating

group, 60.5% in the oxaliplatin-treating group, and 73.2% in the combination-treating group) (Fig. 4b). We also detected FANCD2 monoubiquitylation and found that DSF down-regulated the monoubiquitin modification of FANCD2 induced by carboplatin and oxaliplatin, as expected (Fig. 4c), which further confirmed our supposition.

In addition, we investigated the synergistic effect of DSF with another antitumor drug, hydroxyurea, in H1299 and Bel-7402 cells treated with 5 μmol/L DSF and 2.5 μmol/L hydroxyurea alone or simultaneously for 48 h, which is reported to induce DNA damage and activate the FA repair pathway. The combination treatment of DSF and hydroxyurea resulted in increased cell death in H1299 cells (2.6% in the DSF-treating group, 38.7% in the hydroxyurea-treating group, and 62.8% in the combination-treating group) and Bel-7402 cells (5.9% in the DSF-treating group, 33.5% in the hydroxyurea-treating group, and 59.0% in the combination-treating group) (Fig. 4d). Meanwhile, we found that DSF treatment decreased the monoubiquitin modification of FANCD2 induced by hydroxyurea in H1299 cells and Bel-7402 cells (Fig. 4e). In summary, we discovered that DSF exerted a sensitizing effect on DNA damage agents by inhibiting the FA repair pathway of tumor cells by preventing the monoubiquitination of FANCD2 (Fig. 5).

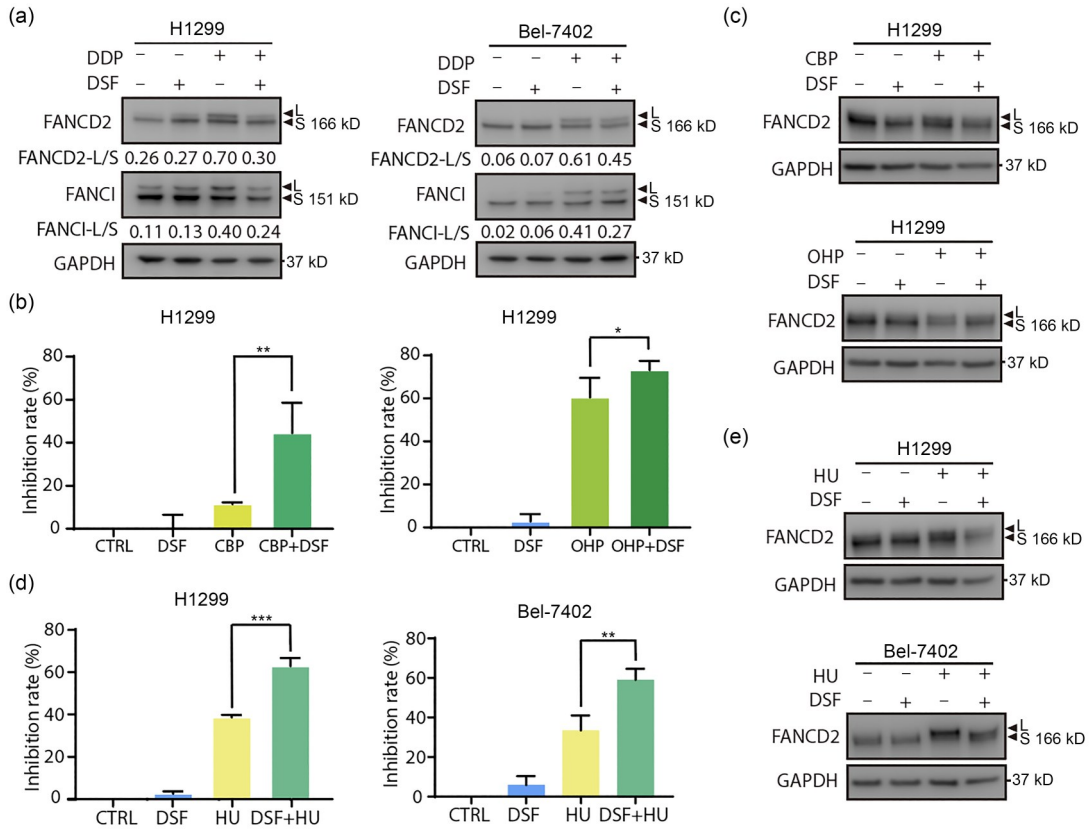

Fig. 4 Antitumor effect of DNA damage agents enhanced by DSF by inhibiting FA repair. (a) Bel-7402 and H1299 cells were treated with 5 μmol/L DSF and 5 μmol/L DDP alone or simultaneously for 24 h. The monoubiquitination levels of FANCD2 and FANCI were determined by western blot. The ratios of monoubiquitination protein to background protein were analyzed by ImageJ. (b) H1299 cells were treated with 10 μmol/L CBP or 5 μmol/L OHP alone or combined with 5 μmol/L DSF for 48 h. Inhibition of proliferation was assessed by the SRB assay. (c) Western blot was preformed to evaluate the changes of the monoubiquitination level of FANCD2 in H1299 cells. (d) H1299 and Bel-7042 cells were treated with 5 μmol/L DSF and 2.5 μmol/L HU alone or simultaneously for 48 h. The proliferation inhibition rate was determined by the SRB assay. (e) Western blot was used to evaluate the changes of the monoubiquitination level of FANCD2 in H1299 and Bel-7402 cells. Data represent the mean±SD, n=3 (* P<0.05, ** P<0.01, *** P<0.001). DDP: cisplatin; DSF: disulfiram; FA: Fanconi anemia; FANCD2: FA complementation group D2; FANCI: FA complementation group I; L: monoubiquitin modification; S: non-ubiquitinated form; GAPDH: glyceraldehyde-3-phosphate dehydrogenase; CBP: carboplatin; OHP: oxaliplatin; SRB: sulforhodamine B; HU: hydroxyurea; SD: standard deviation.

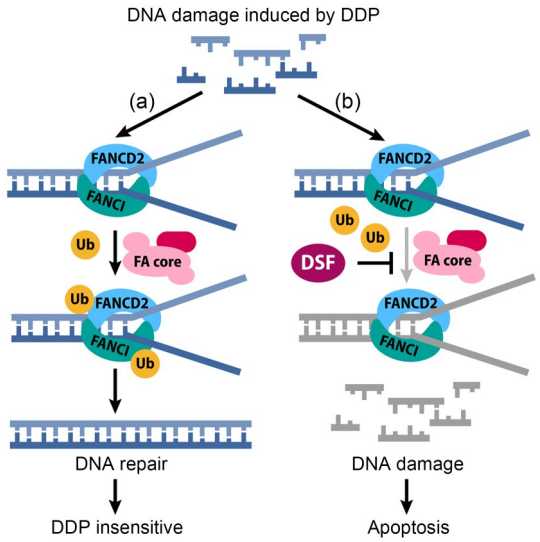

Fig. 5 Schematic diagram of the theory. When DDP-induced DNA damage occurs in tumor cells, (a) intracellular FANCI: FANCD2 heterodimers can trigger the initiation of the FA repair pathway after its monoubiquitination. As a result, some tumor cells are insensitive to the DNA-damaging effects of DDP. (b) DSF can block the monoubiquitination of FANCI: FANCD2 heterodimers, inhibiting the FA repair pathway and reducing the ability of tumor cells to resist DNA damage. DDP: cisplatin; FA: Fanconi anemia; FANCI: FA complementation group I; FANCD2: FA complementation group D2; DSF: disulfiram; Ub: ubiquitin.

4 Discussion

As a potential adjuvant for antitumor drugs, DSF has been validated in clinical trials of various malignant tumors: in combination with copper supplementation in the treatment of metastatic breast cancer, prostate cancer, and refractory liver cancer (Zhang et al., 2010; Galluzzi et al., 2012); in combination with temozolomide in the treatment of recurrent glioblastoma cell tumor; in combination with zinc chelators for melanoma (Zirjacks et al., 2021); and in combination with gemcitabine for metastatic pancreatic cancer (Kim et al., 2013). A phase II clinical trial involving 42 patients with stage IV non-small cell lung cancer showed that DSF with DDP or vinorelbine prolonged the survival of patients by 41% compared with chemotherapy (Nechushtan et al., 2015). However, the molecular mechanism underlying the synergistic antitumor effect of DDP in combination with DSF has not been clarified. Kita et al. (2019) reported that the combination of DSF and DDP resulted in increased DNA-platinum adducts to induce apoptosis, possibly by intervening in the cellular localization of the copper transporter ATPase copper transporting α (ATP7A) in bladder cancer cells, but this was not tested in other tumor cells. The hypothesis we proposed could be verified for a variety of tumor cells based on our study, indicating that the mechanism may be universal. This suggests that the adjuvant effect of DSF could be extended to more cancer types to reduce DDP resistance or toxicity. In our study, we focused mainly on the antitumor activity of DDP in combination with DSF. This treatment appeared to weaken the DNA repair pathway in tumor cells, thereby exacerbating DNA damage induced by DDP within tumor cells. Based on our results, the combination of DDP and DSF can improve the effect of DDP administration, maintain high antitumor activity with a low dose, and reduce other DDP-induced side effects. We used conventional tumor cells in our study and found that the FA repair pathway was involved. Other studies of DSF and DDP have focused on DDP resistance and used DDP-resistant tumor cell lines (Min et al., 2010; Liu et al., 2021; Nakano et al., 2021). In addition to the different types of cancer studied, different hypotheses allow us to discover different underlying mechanisms.

DSF exerts alcohol withdrawal effects by inhibiting ALDH activity to make acetaldehyde accumulate. Moreover, ALDH has been proved to be a functional marker of cancer stem-like cells and ROS. Thus, it was initially considered that the antitumor effect of DSF was attributable to its intervention in ALDH activity. However, it was not clear at first whether the inhibition of ALDH was caused by DSF or its metabolites. A chemical P450 inhibitor can block the downstream metabolism of DSF, causing the generation of a few metabolites. Surprisingly, no inhibition of ALDH was observed when DSF metabolism was blocked, thus confirming that DSF metabolites rather than DSF itself exert the inhibitory effect on ALDH. Later, Majera et al. (2020) discovered that the copper metabolite (CuET) of DSF was responsible for antitumor effects by targeting NPL4 rather than ALDH inhibition. In addition, there are no published studies on the antitumor activity of DSF metabolites that target ALDH. Therefore, we examined the combination of DSF with NCT-501, a reported ALDH inhibitor, in H1299 cells and found that NCT-501 did not promote the antitumor effect of DDP like DSF (data not shown). Therefore, we concluded that the toxicity of DSF in tumor cells might have nothing to do with ALDH inhibition.

This provided a new clue to re-assess the role of ALDH as a potential antitumor target of DSF and thereby contributed to solving the often-misunderstood findings in this field.

At present, the DNA damage induced by radiotherapy, chemotherapy, and PARP inhibitors in tumor cells is a general strategy for the treatment of various types of tumors. However, there are different pathways to repair DNA damage, including base excision repair, NER, mismatch repair, FA repair, homologous recombination repair, and non-homologous end joining repair, which may result in tumor cells gradually becoming resistant. DDP is a clinically common chemotherapy drug, but induces several toxic responses with the increase of dosage in bone marrow, gastrointestinal renal tissues, nerves, etc. Thus, it is of great importance to reverse drug resistance and reduce the dose of DDP via combined therapy. As a DNA crosslinker, DDP has been reported to repair DNA damage mainly through the NER and FA repair pathways. Our findings indicated that DSF significantly enhanced the inhibition of proliferation and induction of apoptosis by DDP by inhibiting the FA repair pathway in some types of tumor cells. Further research on the upstream pathway of FANCD2-FANCI monoubiquitylation is needed. Furthermore, we found that DSF could sensitize tumor cells to chemotherapeutics that activate the FA repair pathway including carboplatin, oxaliplatin, and hydroxyurea in the same way, providing support for expanding the application range of DSF in combination treatment of tumors and revealing the potential of DSF to reverse drug resistance. Here, only the method of RNA sequencing (RNA-seq) was performed to obtain information at the gene level. We believe that with the further research, other methods like protein mass spectrometry can be used to verify our current results and obtain more information (Chen and Chen, 2021; Zhong et al., 2021).

Taken together, we first found that DSF had a synergistic antitumor effect with DDP by inhibiting the FA repair pathway to increase DNA damage. Moreover, we discovered that DSF could similarly enhance the antitumor activity of carboplatin, oxaliplatin, and hydroxyurea, suggesting that the molecular mechanism of the sensitizing effect of DSF is through inhibiting the FA repair pathway. In conclusion, our study provides new possibilities for repurposing DSF for application in combined tumor therapies.

Acknowledgments

The work was supported by the National Natural Science Foundation of China (No. 82104192), the Zhejiang Provincial Natural Science Foundation (No. LR22H310002), the Scientific Research Fund of Zhejiang University (No. XY2021044), and the Zhejiang University K. P. Chao's High Technology Development Foundation.

Author contributions

Meng YUAN, Qian WU, Mingyang ZHANG, Minshan LAI, and Wenbo CHEN performed the experimental research and data analysis. Meng YUAN, Qian WU, and Minshan LAI wrote and edited the manuscript. Jianfeng YANG, Li JIANG, and Ji CAO contributed to the study design, writing, and editing of the manuscript. All authors have read and approved the final manuscript, and therefore, have full access to all the data in the study and take responsibility for the integrity and security of the data.

Compliance with ethics guidelines

Meng YUAN, Qian WU, Mingyang ZHANG, Minshan LAI, Wenbo CHEN, Jianfeng YANG, Li JIANG, and Ji CAO declare that they have no conflict of interest.

This article does not contain any studies with human or animal subjects performed by any of the authors.

References

Bai ZS, Peng YL, Ye XY, et al., 2022. Autophagy and cancer treatment: four functional forms of autophagy and their therapeutic applications. *J Zhejiang Univ-Sci B (Biomed & Biotechnol)*, 23(2):89-101. https://doi.org/10.1631/jzus.B2100804

Brabec V, Nováková O, 2006. DNA binding mode of ruthenium complexes and relationship to tumor cell toxicity. *Drug Resist Updat*, 9(3):111-122. https://doi.org/10.1016/j.drup.2006.05.002

Castella M, Jacquemont C, Thompson EL, et al., 2015. FANCI regulates recruitment of the FA core complex at sites of DNA damage independently of FANCD2. *PLoS Genet*, 11(10):e1005563. https://doi.org/10.1371/journal.pgen.1005563

Chen SY, Chang YL, Liu ST, et al., 2021. Differential cytotoxicity mechanisms of copper complexed with disulfiram in oral cancer cells. *Int J Mol Sci*, 22(7):3711. https://doi.org/10.3390/ijms22073711

Chen Z, Chen JJ, 2021. Mass spectrometry-based protein–protein interaction techniques and their applications in studies of DNA damage repair. *J Zhejiang Univ-Sci B (Biomed & Biotechnol)*, 22(1):1-20. https://doi.org/10.1631/jzus.B2000356

Fang L, Qi H, Wang P, et al., 2022. UPF1 increases amino acid levels and promotes cell proliferation in lung adenocarcinoma via the eIF2α-ATF4 axis. *J Zhejiang Univ-Sci B (Biomed & Biotechnol)*, 23(10):863-875. https://doi.org/10.1631/jzus.B2200144

Feng YL, Liu SC, Chen RD, et al., 2021. Target binding and residence: a new determinant of DNA double-strand break repair pathway choice in CRISPR/Cas9 genome editing. *J Zhejiang Univ-Sci B (Biomed & Biotechnol)*, 22(1):73-86. https://doi.org/10.1631/jzus.B2000282

Galluzzi L, Senovilla L, Vitale I, et al., 2012. Molecular mechanisms of cisplatin resistance. *Oncogene*, 31(15):1869-1883. https://doi.org/10.1038/onc.2011.384

Guo LM, Cui J, Wang HR, et al., 2021. Metformin enhances anti-cancer effects of cisplatin in meningioma through AMPK-mTOR signaling pathways. *Mol Ther Oncolytics*, 20:119-131. https://doi.org/10.1016/j.omto.2020.11.004

Halatsch ME, Kast RE, Karpel-Massler G, et al., 2021. A phase Ib/IIa trial of 9 repurposed drugs combined with temozolomide for the treatment of recurrent glioblastoma: CUSP9v3. *Neuro-Oncol Adv*, 3(1):vdab075. https://doi.org/10.1093/noajnl/vdab075

Ishiai M, 2021. Regulation of the fanconi anemia DNA repair pathway by phosphorylation and monoubiquitination. *Genes*, 12(11):1763. https://doi.org/10.3390/genes12111763

Jangra A, Choi SA, Yang J, et al., 2020. Disulfiram potentiates the anticancer effect of cisplatin in atypical teratoid/rhabdoid tumors (AT/RT). *Cancer Lett*, 486:38-45. https://doi.org/10.1016/j.canlet.2020.05.006

Kim SK, Kim H, Lee DH, et al., 2013. Reversing the intractable nature of pancreatic cancer by selectively targeting ALDH-high, therapy-resistant cancer cells. *PLoS ONE*, 8(10):e78130. https://doi.org/10.1371/journal.pone.0078130

Kita Y, Hamada A, Saito R, et al., 2019. Systematic chemical screening identifies disulfiram as a repurposed drug that enhances sensitivity to cisplatin in bladder cancer: a summary of preclinical studies. *Br J Cancer*, 121(12):1027-1038. https://doi.org/10.1038/s41416-019-0609-0

Lee JO, Kang MJ, Byun WS, et al., 2019. Metformin overcomes resistance to cisplatin in triple-negative breast cancer (TNBC) cells by targeting RAD51. *Breast Cancer Res*, 21:115. https://doi.org/10.1186/s13058-019-1204-2

Liang ZR, Zhang T, Zhan T, et al., 2021. Metformin alleviates cisplatin-induced ototoxicity by autophagy induction possibly via the AMPK/FOXO3a pathway. *J Neurophysiol*, 125(4):1202-1212. https://doi.org/10.1152/jn.00417.2020

Liu CC, Wu CL, Lin MX, et al., 2021. Disulfiram sensitizes a therapeutic-resistant glioblastoma to the TGF-β receptor inhibitor. *Int J Mol Sci*, 22(19):10496. https://doi.org/10.3390/ijms221910496

Majera D, Skrott Z, Chroma K, et al., 2020. Targeting the NPL4 adaptor of p97/VCP segregase by disulfiram as an emerging cancer vulnerability evokes replication stress and DNA damage while silencing the ATR pathway. *Cells*, 9(2):469. https://doi.org/10.3390/cells9020469

Makovec T, 2019. Cisplatin and beyond: molecular mechanisms of action and drug resistance development in cancer chemotherapy. *Radiol Oncol*, 53(2):148-158. https://doi.org/10.2478/raon-2019-0018

Min KA, Yu FQ, Yang VC, et al., 2010. Transcellular transport of heparin-coated magnetic iron oxide nanoparticles (Hep-MION) under the influence of an applied magnetic field. *Pharmaceutics*, 2(2):119-135. https://doi.org/10.3390/pharmaceutics2020119

Nakano T, Warner KA, Oklejas AE, et al., 2021. mTOR inhibition ablates cisplatin-resistant salivary gland cancer stem cells. *J Dent Res*, 100(4):377-386. https://doi.org/10.1177/0022034520965141

Nechushtan H, Hamamreh Y, Nidal S, et al., 2015. A phase IIb trial assessing the addition of disulfiram to chemotherapy for the treatment of metastatic non-small cell lung cancer. *Oncologist*, 20(4):366-367. https://doi.org/10.1634/theoncologist.2014-0424

Park YM, Go YY, Shin SH, et al., 2018. Anti-cancer effects of disulfiram in head and neck squamous cell carcinoma via autophagic cell death. *PLoS ONE*, 13(9):e0203069. https://doi.org/10.1371/journal.pone.0203069

Qi X, Yan DH, Zuo JC, et al., 2021. Development of a novel chemokine signaling-based multigene signature to predict prognosis and therapeutic response in colorectal cancer. *J Zhejiang Univ-Sci B (Biomed & Biotechnol)*, 22(12):1053-1059. https://doi.org/10.1631/jzus.B2100412

Ren XY, Li YC, Zhou Y, et al., 2021. Overcoming the compensatory elevation of NRF2 renders hepatocellular carcinoma cells more vulnerable to disulfiram/copper-induced ferroptosis. *Redox Biol*, 46:102122. https://doi.org/10.1016/j.redox.2021.102122

Rocha CRR, Silva MM, Quinet A, et al., 2018. DNA repair pathways and cisplatin resistance: an intimate relationship. *Clinics*, 73(S1):e478s. https://doi.org/10.6061/clinics/2018/e478s

Schmidtova S, Kalavska K, Gercakova K, et al., 2019. Disulfiram overcomes cisplatin resistance in human embryonal carcinoma cells. *Cancers*, 11(9):1224. https://doi.org/10.3390/cancers11091224

Skrott Z, Mistrik M, Andersen KK, et al., 2017. Alcohol-abuse drug disulfiram targets cancer via p97 segregase adaptor NPL4. *Nature*, 552(7684):194-199. https://doi.org/10.1038/nature25016

Skrott Z, Majera D, Gursky J, et al., 2019. Disulfiram's anticancer activity reflects targeting NPL4, not inhibition of aldehyde dehydrogenase. *Oncogene*, 38(40):6711-6722. https://doi.org/10.1038/s41388-019-0915-2

Smogorzewska A, Matsuoka S, Vinciguerra P, et al., 2007. Identification of the FANCI protein, a monoubiquitinated FANCD2 paralog required for DNA repair. *Cell*, 129(2):289-301. https://doi.org/10.1016/j.cell.2007.03.009

Wang K, Michelakos T, Wang B, et al., 2021. Targeting cancer stem cells by disulfiram and copper sensitizes radioresistant chondrosarcoma to radiation. *Cancer Lett*, 505:37-48.

https://doi.org/10.1016/j.canlet.2021.02.002

Wu Q, Zhang MY, Wen YM, et al., 2022. Identifying chronic alcoholism drug disulfiram as a potent DJ-1 inhibitor for cancer therapeutics. *Eur J Pharmacol*, 926:175035. https://doi.org/10.1016/j.ejphar.2022.175035

Xia L, Lin HX, Zhou YM, et al., 2022. ZNF750 facilitates carcinogenesis via promoting the expression of long non-coding RNA *CYTOR* and influences pharmacotherapy response in colon adenocarcinoma. *J Zhejiang Univ-Sci B (Biomed & Biotechnol)*, 23(7):587-596. https://doi.org/10.1631/jzus.B2100939

Xu YQ, Zhou Q, Feng XL, et al., 2020. Disulfiram/copper markedly induced myeloma cell apoptosis through activation of JNK and intrinsic and extrinsic apoptosis pathways. *Biomed Pharmacother*, 126:110048. https://doi.org/10.1016/j.biopha.2020.110048

Yang YY, Lindsey-Boltz LA, Vaughn CM, et al., 2021. Circadian clock, carcinogenesis, chronochemotherapy connections. *J Biol Chem*, 297(3):101068. https://doi.org/10.1016/j.jbc.2021.101068

Yang Z, Guo F, Albers AE, et al., 2019. Disulfiram modulates ROS accumulation and overcomes synergistically cisplatin resistance in breast cancer cell lines. *Biomed Pharmacother*, 113:108727. https://doi.org/10.1016/j.biopha.2019.108727

Yarde DN, Oliveira V, Mathews L, et al., 2009. Targeting the Fanconi anemia/BRCA pathway circumvents drug resistance in multiple myeloma. *Cancer Res*, 69(24):9367-9375. https://doi.org/10.1158/0008-5472.CAN-09-2616

Zhang HJ, Chen D, Ringler J, et al., 2010. Disulfiram treatment facilitates phosphoinositide 3-kinase inhibition in human breast cancer cells *in vitro* and *in vivo*. *Cancer Res*, 70(10):3996-4004. https://doi.org/10.1158/0008-5472.CAN-09-3752

Zhao LJ, Teng B, Wen LJ, et al., 2014. mTOR inhibitor AZD8055 inhibits proliferation and induces apoptosis in laryngeal carcinoma. *Int J Clin Exp Med*, 7(2):337-347.

Zhong WW, Wang DJ, Yao B, et al., 2021. Integrative analysis of prognostic long non-coding RNAs with copy number variation in bladder cancer. *J Zhejiang Univ-Sci B (Biomed & Biotechnol)*, 22(8):664-681. https://doi.org/10.1631/jzus.B2000494

Zirjacks L, Stransky N, Klumpp L, et al., 2021. Repurposing disulfiram for targeting of glioblastoma stem cells: an in vitro study. *Biomolecules*, 11(11):1561. https://doi.org/10.3390/biom11111561

Supplementary information

Figs. S1 and S2